Highly sensitive and efficient hydrazine sensor probe development based on MoO3/CuO/ZnO ternary mixed metal oxide nano-composites for sustainable environment

Author

Subhan, Md Abdus, Saha, Pallab Chandra, Akand, Mohammad Arifur Rahman, Asiri, Abdullah M, Al#Mamun, Mohammad, Rahman, Mohammed M

Published

2022

Journal Title

Electrochemical Science Advances

Version

Version of Record (VoR)

DOI

10.1002/elsa.202100031

Full article
doi.org/10.1002/elsa.202100031

Chemistry Europe
European Chemical Societies Publishing

Received: 26 February 2021
Revised: 21 March 2021
Accepted: 23 March 2021

Highly sensitive and efficient hydrazine sensor probe development based on MoO_3/CuO/ZnO ternary mixed metal oxide nano-composites for sustainable environment

Md Abdus Subhan[1] | **Pallab Chandra Saha**[1] | **Mohammad Arifur Rahman Akand**[1] | **Abdullah M. Asiri**[2] | **Mohammad Al-Mamun**[3] | **Mohammed M. Rahman**[2]

[1] Department of Chemistry, Shah Jalal University of Science and Technology, Sylhet 3114, Bangladesh

[2] Center of Excellence for Advanced Materials Research (CEAMR), Department of Chemistry, Faculty of Science, King Abdulaziz University, Jeddah, Saudi Arabia

[3] Centre for Clean Environment and Energy, Griffith School of Environment, Gold Coast Campus, Griffith University, Queensland, Australia

Correspondence
Dr. Md Abdus Subhan, Professor of the Department of Chemistry, Shahjalal University of Science and Technology, Sylhet 3114, Bangladesh.
Email: subhan-che@sust.edu
Dr. Mohammed M. Rahman, Professor, Center of Excellence for Advanced Materials Research (CEAMR) & Chemistry Department, Faculty of Science, King Abdulaziz University, Jeddah 21589, P.O. Box 80203, Saudi Arabia.
Email: mmrahman@kau.edu.sa and mmrahmanh@gmail.com

Abstract

In this study, by using a co-precipitation method MoO_3/CuO/ZnO nanocomposite material was synthesized. Then the prepared material was fully characterized by using XRD (X-ray diffraction), SEM (scanning electron microscopy), EDS (energy dispersive x-ray spectroscopy), CV (cyclic voltammetry), and EIS (Electrochemical Impedance Spectroscopy). Zeta potential and hydrodynamic size were measured using a Zetasizer in PBS buffer. By using Scherrer's formula from XRD, particle size was determined which was around 26.5 nm. For the promising chemical sensor development, MoO_3/CuO/ZnO nanocomposite material was fabricated onto a glassy carbon electrode (GCE) to provide a sensor probe with a fast response towards the selective hydrazine (HZ) toxin in phosphate buffer phase. The fabricated sensor probe is exhibited good sensitivity and long-term stability as well as enhanced electrochemical performances. A calibration plot was found linear in the range of 0.2 nM to 2.0 mM (linear dynamic range, LDR) in presence of aqueous HZ solutions with highest sensitivity value and lower limit of detection and good limit of quantification (LOQ). This approach is promising as an efficient technique in developing a highly effective sensor probe with ternary metal oxides for detecting environmental pollutants on a broad scale.

KEYWORDS
electro-chemical method, environmental safety, fabrication, hydrazine detection, MoO3/CuO/ZnO nanomaterials

1 | INTRODUCTION

Metal oxide nanomaterial is used as an emerging and promising electro-catalyst. Doping in a metal oxide nanomaterial produced strain into the lattice of the host through defects in the structure. The lattice of the oxide host causes a non-typical coordination environment on the dopant, which subsequently perturbed the dopant electronic properties. Thus, mixed metal oxides facilitate the creation of new oxidation states, which are absent in mono-metal oxides.[1] Mixed metal trimetallic oxide nanocomposites with different oxides, for instance, ZnO, MoO_3, and CuO

Full article
doi.org/10.1002/elsa.202100031
Chemistry Europe
European Chemical Societies Publishing

are excellent candidates for photocatalytic applications, environmental protections, toxin sensor, an efficient antibacterial agent against MDR pathogenic bacteria as well as an industrial sterilization material.[2–7]

Hydrazine is an environmental toxin, which is a carcinogenic, poisonous, hazardous, cyanogenetic, and nephrotoxic material.[8] Many applications of hydrazine hydrates are found in insecticides, regulators in plant-growth, dyes as well as photographic industries, drug as well as pharmaceuticals and polymer industry, agro-industries, rocket fuel, space craft's fuel, and explosives.[9] Irritation in eyes and nose, short-term loss of sight, fainting, vomiting, respiratory edema, loss of liver and kidney functions, and unconsciousness are the symptoms of high exposure to hydrazine.[10] Absorbed HZ into the skin creates burning and impede the blood production.[11] Thus, developing an advanced analytical technique for the detection and determination of HZ is highly demanding. A hydrazine chemi-sensor based on sulfur-doped γ-MnOOH microrods coated GCE, and palladium nanoparticle coated gaur gum-based composite for electrochemical detection of hydrazine hydrate have been reported.[12,13] The electrochemical sensors are always found as a rapid, powerful, and cost-effective method for HZ detection and determination. There have been numerous studies for the modified electrodes, which increased the rate of electron transfer as well as reduced the high potential of the HZ oxidation.[14–18] To improve sensor matrixes, the redox mediators including metal and metal oxide nanoparticles, organic-mediators, hexacyanoferrate salts, etc. have been used.[14–22] The HZ detection methods have also been reported by many researchers.[23–33] However, these conventional techniques are either highly costly, time consuming, or require expensive instruments to execute. Usually, these methods are not suitable for detection of very low, nM concentration of HZ. During the electrochemical detection of ultra-trace amount of environmental unsafe toxins, nanostructured materials exhibited better properties than their bulk one.[34]

Generally, doped materials have employed a great deal of consideration due to their chemical, structural, physical, and optical properties in terms of large-active surface area, high-stability, high porosity, and permeability, which directly depends on the structural morphology, prepared by reactant precursors with co-precipitation method in basic medium at room temperature.[2–7] This technique has several advantages including facile preparation, accurate control of the reactant temperature, easy to handle, one-step reaction, and high-porosity as well as porous natures of ternary doped materials compared to un-doped counterparts. Optical, morphological, electrical, and chemical properties of ternary nanomaterials are of huge significance from the scientific aspect compared to other un-doped materials.[35–37] Non-stoichiometry, mostly oxygen vacancies, makes it conducting nature in the doped nanomaterials. The formation energy of oxygen vacancies and metal interstitials in ternary doped material is very low and thus these defects form readily, resulting in the experimentally elevated conductivity of MoO_3/CuO/ZnO nanostructure materials compared to undoped MoO_3, CuO, ZnO individuals.[38,39] Therefore, MoO_3/CuO/ZnO nanomaterials have fascinated significant attention owing to their potential applications in constructing opto-electronics, electro-analytical selective detection assays, sensor devices, hybrid-composites, electron-field emission sources for emission exhibits, biochemical detections, and Surface-Enhanced Raman properties. MoO_3/CuO/ZnO nanomaterial offers improved performance in detection of hydrazine. Because the large-active surface area has increased the conductivity as well as current responses of MoO_3/CuO/ZnO nanomaterials/Nafion/GCE assembly during the electrochemical study.

Preparation of nanostructure materials by co-precipitation method is facile and cost effective relative to other methods.[37] Herein, a sensitive electrochemical sensor has been developed by MoO_3/CuO/ZnO nanomaterials fabricated GCE for selective detection and determination of HZ in aqueous solution using the modest electrochemical methods.[40,41] Out of all the recent electro-chemical detection approaches, the two electrodes system electrochemical technique exhibits a chance for a practical, inexpensive and rapid detection of HZ. As far as we are aware, MoO_3/CuO/ZnO nanomaterials fabricated nafion/GCE sensor has not yet been reported. In this work, a potential application for the determination of HZ using fabricated MoO_3/CuO/ZnO nanomaterials/nafion/GCE has been reported.

2 | RESULTS AND DISCUSSION

2.1 | 2.1 Characterization of MoO_3/CuO/ZnO nanomaterials

Figure 1 represents XRD pattern of the synthesized MoO_3/CuO/ZnO composites. The XRD was measured to know the compositions and phases of the nanocomposite. The peaks at $2\theta = 25.78°$, 28.45°, 30.30°, 35.74°, 38.00°, and 66.70° are due to MoO_3 supported by JCPDS No. 05–0508. Peaks at 32.93°, 35.74°, 38.00°, 48.19°, 58.03°, 63.50°, 66.70°, and 68.80° confirms the CuO formation, which is consistent with JCPDS No. 05–0661. Peaks at $2\theta = 30.30°$, 32.93°, 35.74°, 48.19°, 58.03°, 63.50°, 66.70°, and 68.80° are corresponding to ZnO structure according to JCPDS No.

Full article
doi.org/10.1002/elsa.202100031
Chemistry Europe
European Chemical Societies Publishing

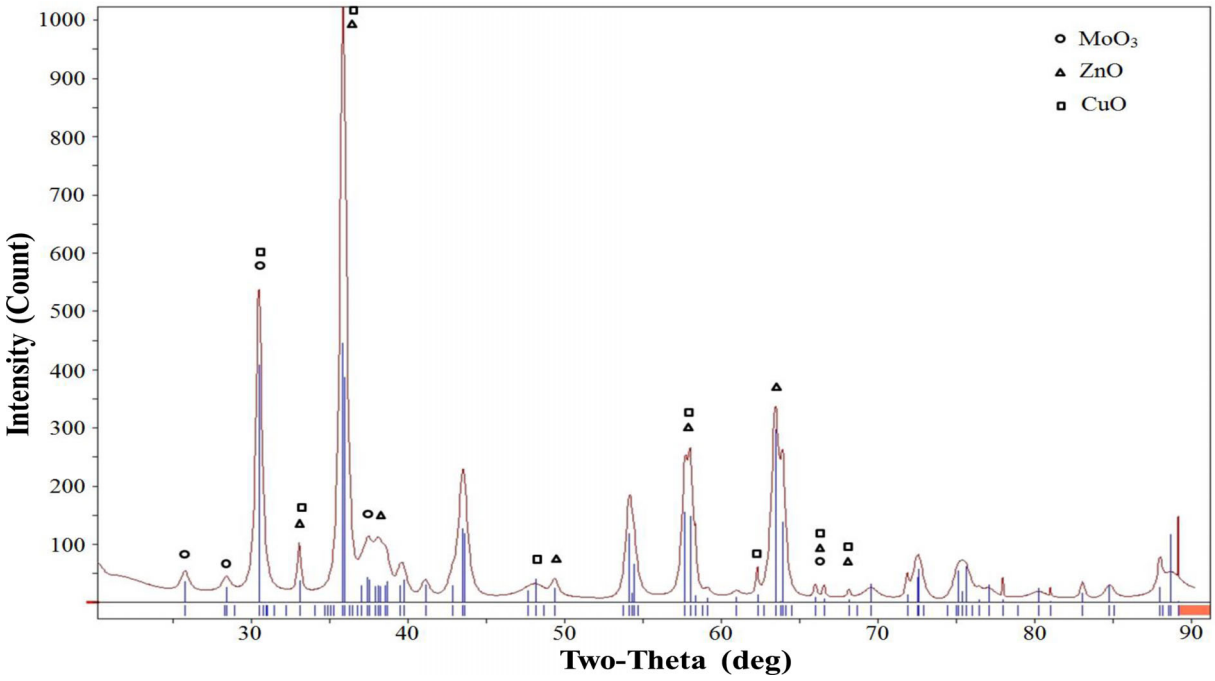

FIGURE 1 The XRD pattern of ternary MoO_3/CuO/ZnO nanomaterials for the study of crystallinity

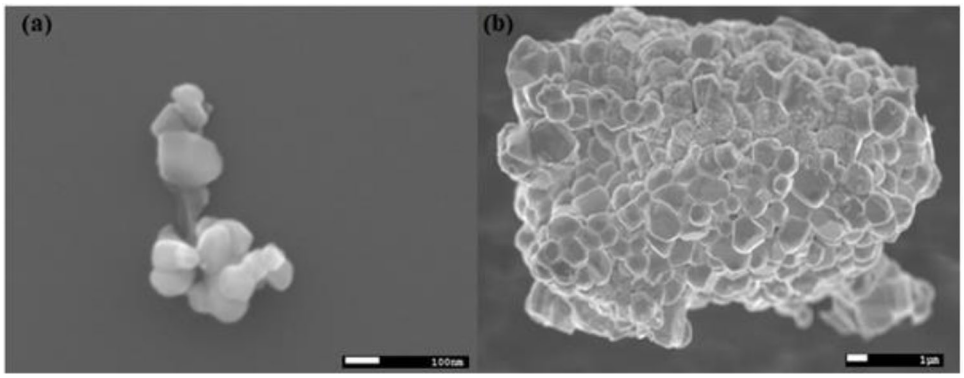

FIGURE 2 SEM images of MoO_3/CuO/ZnO nanomaterials at different magnificent to examine the morphology of prepared sample

36–1451. The estimated size of particles was about 26.5 nm by Scherrer formula.[42]

$$\tau = K\lambda/(\beta \cos\theta)$$

Here, τ is the mean size, K is the shape factor with a value 0.94 (dimensionless), λ is the x-ray wavelength of 0.1506 nm, β is the line broadening at half of the maximum intensity (FWHM) and θ is the Bragg angle.

2.2 | The analysis of SEM and EDS of MoO_3/CuO/ZnO nanomaterials

MoO_3/CuO/ZnO particles were characterized by SEM and EDS measurement to reveal the surface characteristics, morphology and elemental compositions.[7] The SEM image (Figure 2) shows that the particles are in an agglomerated form with irregular rhombohedral and monoclinic morphologies. Although agglomerated, the individual particles are clearly seen in SEM images. The EDS measurement (Fig S1) proved the presence of molybdenum (Mo), copper (Cu), zinc (Zn), and oxygen (O) with a percentage of 1.42, 9.67, 28.45, and 60.46 respectively.

2.3 | Hydrodynamic size and zeta potential MoO_3/CuO/ZnO nanomaterials

For the analysis of the size and charge in dispersed media, hydrodynamic size and zeta potential of MoO_3/CuO/ZnO

Full article
doi.org/10.1002/elsa.202100031
Chemistry Europe
European Chemical Societies Publishing

TABLE 1 Hydro-dynamic size and zeta potential of MoO_3/CuO/ZnO nanomaterial

Compound	Na-citrate buffer (pH 4.95)			PBS buffer (pH 7.4)		
MoO_3/CuO/ZnO nanomaterials	Size (nm)	Zeta potential	PDI	Size (nm)	Zeta potential	PDI
	829	−21.30	0.42	1217	−6.55	0.78

nanomaterial were studied in acidic and basic pH in Na-citrate and PBS buffer system, respectively. Hydro-dynamic size, zeta potential, and poly dispersive index (PDI) have been listed in Table 1. The hydro-dynamic size of MoO_3/CuO/ZnO nanomaterial in acidic pH was observed to be 829.0 nm and in basic pH 1217.0 nm. Zeta potential in acidic pH has been observed to be −21.3 meV, whereas in basic pH −6.55. The results are indicated the overall negatively charged MoO_3/CuO/ZnO particles in the dispersed media either in acidic or basic pH condition.

3 | APPLICATION

3.1 | Detection of HZ using MoO_3/CuO/ZnO nanomaterials by electrochemical method

The MoO_3/CuO/ZnO nanomaterials/Nafion/GCE, sensors have several plus points such as electro-chemical activity and safe characteristics. As in the case of HZ sensors, the current response in electrochemical method of MoO_3/CuO/ZnO nanomaterials/Nafion/GCE changes when aqueous HZ analyte is adsorbed (Figure 3). The MoO_3/CuO/ZnO nanomaterials/Nafion/GCE is applied for fabrication of chemo-sensor, where HZ is measured as target analyte. The fabricated-surface of MoO_3/CuO/ZnO nanomaterials/Nafion/GCE sensor was prepared with conducting binder (5% Nafion) on the flat-surface. Electro-chemical signals of HZ chemical sensor are predicted having MoO_3/CuO/ZnO nanomaterials/Nafion/GCE on thin-film as a function of current versus potential. The resultant electrical responses of target HZ are evaluated by simple as well as reliable electrochemical method by using MoO_3•CuO•ZnO nanomaterials/Nafion/GCE. 1.0 s holding time was set for the electrometer. A major amplification in the current response with applied potential was established.

The aqueous HZ sensing mechanism onto MoO_3/CuO/ZnO nanomaterials/Nafion/GCE probe is based on the ternary metal oxides, due to adsorption/absorption of aqueous oxygen onto the surface of MoO_3/CuO/ZnO nanomaterials itself, according to the dissolved O_2 in bulk-solution or surface-air of the surrounding atmosphere (Equation i-iii). These reactions are taken place in bulk-solution or air/liquid interface or surrounding air due to the low carrier concentration, which probably increased the resistance of material surface as well as decreased the conductivity.[43–45] The analyte sensitivity towards MoO_3/CuO/ZnO nanomaterials could be attributed to the high oxygen deficiency and defect density, which leads to increase the oxygen adsorption for forming active species as O_2^-, then O^- and finally OH^-. The larger the amount of oxygen adsorbed on the MoO_3/CuO/ZnO nanomaterials surface, the larger the oxidizing capability. The larger the oxidizing ability of the material, the faster would be the oxidation of selective HZ.

$$\mathbf{e^-}(\text{onto } MoO_3/CuO/Zn\ Osurface) + \mathbf{O_2} \rightarrow \mathbf{O_2^-} \quad \text{(i)}$$

$$\mathbf{e^-}(\text{onto } MoO_3/CuO/Zn\ Osurface) + \mathbf{O_2^-} \rightarrow \mathbf{2O^-} \quad \text{(ii)}$$

$$\mathbf{O^-}(\text{onto } MoO_3/CuO/Zn\ Osurface) + \mathbf{H_2O} \rightarrow \mathbf{2OH^-} \quad \text{(iii)}$$

Then, the oxidation reaction of HZ onto MoO_3/CuO/ZnO nanomaterials/Nafion/GCE in the buffer system is proposed and presented below according to equation (iv). According to the electrochemical oxidation process, targeted HZ molecule is oxidized, hence released the electrons, which is presented in schematic representation (Scheme 1). Therefore, the electrochemical response is increased significantly with the MoO_3/CuO/ZnO nanomaterials/Nafion/GCE sensor probe in the electro-chemical system. Finally, in contact with the MoO_3/CuO/ZnO nanomaterials surface, HZ is oxidized by releasing two electrons on the sensor MoO_3/CuO/ZnO nanomaterials/Nafion/GCE probe surface, which is measured during the electrochemical measurement at room conditions by I-V electrochemical method. Throughout the oxidation of HZ, the current is pointedly improved by producing ammonia in the electro-chemical process. In presence of MoO_3/CuO/ZnO nanomaterials/Nafion/GCE, the electrons are released in contact of HZ by adsorbing the reducing oxygen, which improved and enhanced the current responses against applied potential during the electrochemical measurement at room conditions.[46–48] The electrochemical reaction for the electro-catalytic oxidation of HZ (Reaction iv) is proposed and presented as below (Scheme 1).

$$\mathbf{N_2H_4}(MoO_3/CuO/ZnO/Nafion/GCE) + {}^{5}/_{2}\mathbf{OH^-} \rightarrow {}^{1}/_{2}\mathbf{N^{-3}} + {}^{1}/_{2}\mathbf{NH_3} + {}^{5}/_{2}\mathbf{H_2O} + \mathbf{2e^-} \quad \text{(iv)}$$

Full article
doi.org/10.1002/elsa.202100031
Chemistry Europe
European Chemical Societies Publishing

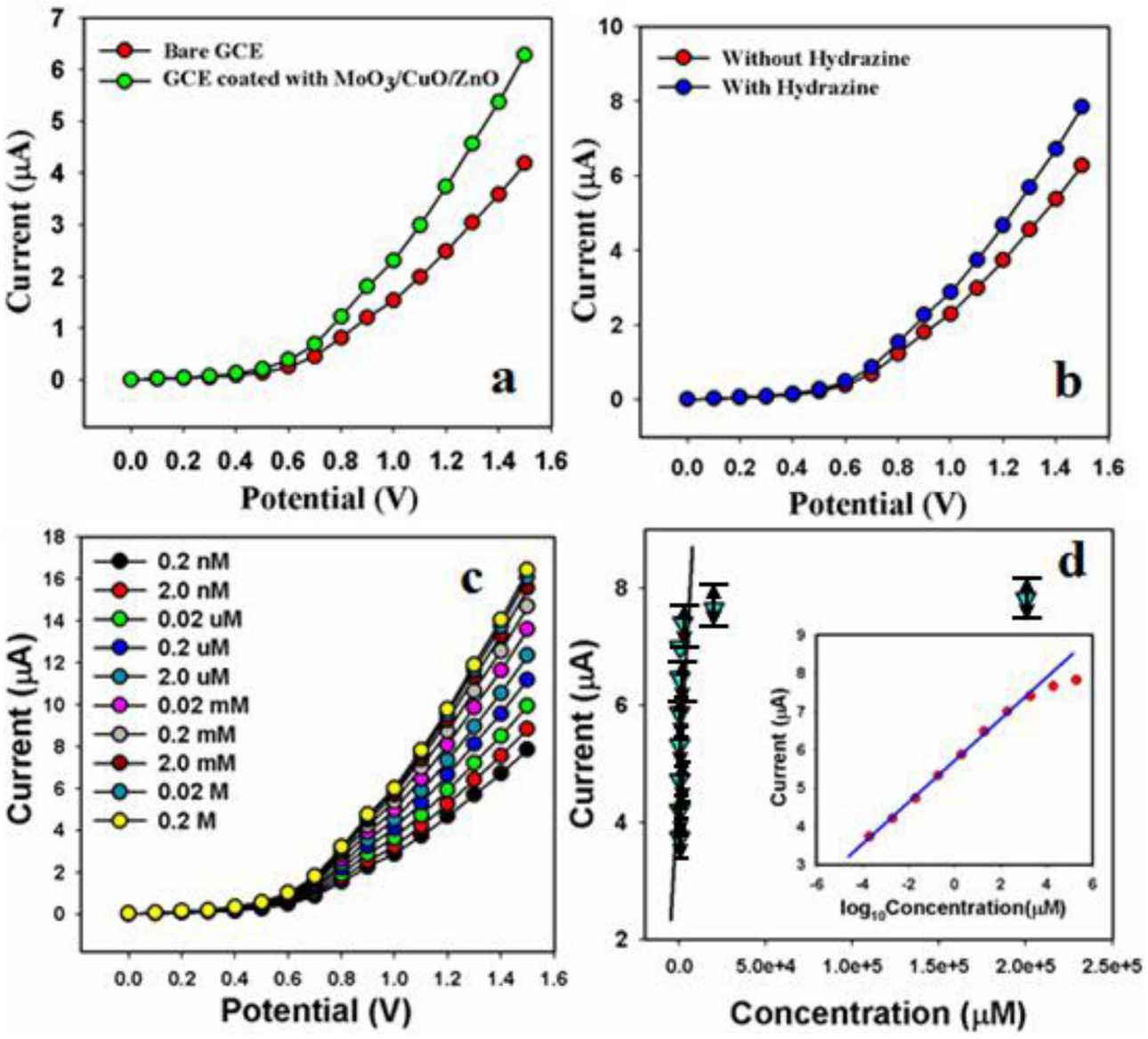

FIGURE 3 Detection of HZ with MoO_3/CuO/ZnO nanomaterials/GCE. (A) Bare GCE electrode (red-dotted) and coated GCE electrode with conducting nafion (5% ethanol) coating binders (green-dotted), (B) Electrochemical responses of the coated GCE without HZ (red-dotted) and with HZ (blue-dotted; 1.0 μM; 25.0 μL) in 5.0 mL of PBS solution, and (C) Current variations for different concentration (0.2 nM to 0.2 M) of aqueous HZ solution in the voltage range 0.0 to +1.5 V and (D) Calibration plot of MoO_3/CuO/ZnO nanomaterials fabricated GCE surfaces at +1.1 V and (Inset) Calibration of MoO_3/CuO/ZnO nanomaterials/GCE with HZ (log-Conc. of HZ vs current)

Ternary doped nanomaterials have been reported as promising chemical sensors with a variety of electroanalytical techniques.[49–53] The significant application of MoO_3/CuO/ZnO nanocomposite materials/Nafion/GCE accumulated onto an electrode as chemical sensor has been utilized to detect environmentally toxic substances. Current response in the electrochemical method for the MoO_3/CuO/ZnO nanomaterials/Nafion/GCE has been significantly changed during the adsorption of HZ as a target agent. In the potential range of 0.1 to 1.5 V, the current responses for the electrode coated with MoO_3/CuO/ZnO nanomaterials/Nafion/GCE on the working electrode surface were significantly used. Presence of toxin HZ in an aqueous solution has been identified as well as determined by MoO_3/CuO/ZnO nanomaterials fabricated GCE as a chemical sensor probe. The nontoxic character, chemical stability, and electrochemical performance are made the MoO_3/CuO/ZnO materials as good sensing materials for the HZ detection. Upon contact with MoO_3/CuO/ZnO nanomaterials, HZ gives a remarkable response, which was observed by the electrochemical method (Figure 3).

Current intensities in PBS (pH = 7.1) without HZ for bare-GCE (red dotted) and MoO_3/CuO/ZnO nanomaterials fabricated GCE (green-dotted) are measured and

Full article
doi.org/10.1002/elsa.202100031
Chemistry Europe
European Chemical Societies Publishing

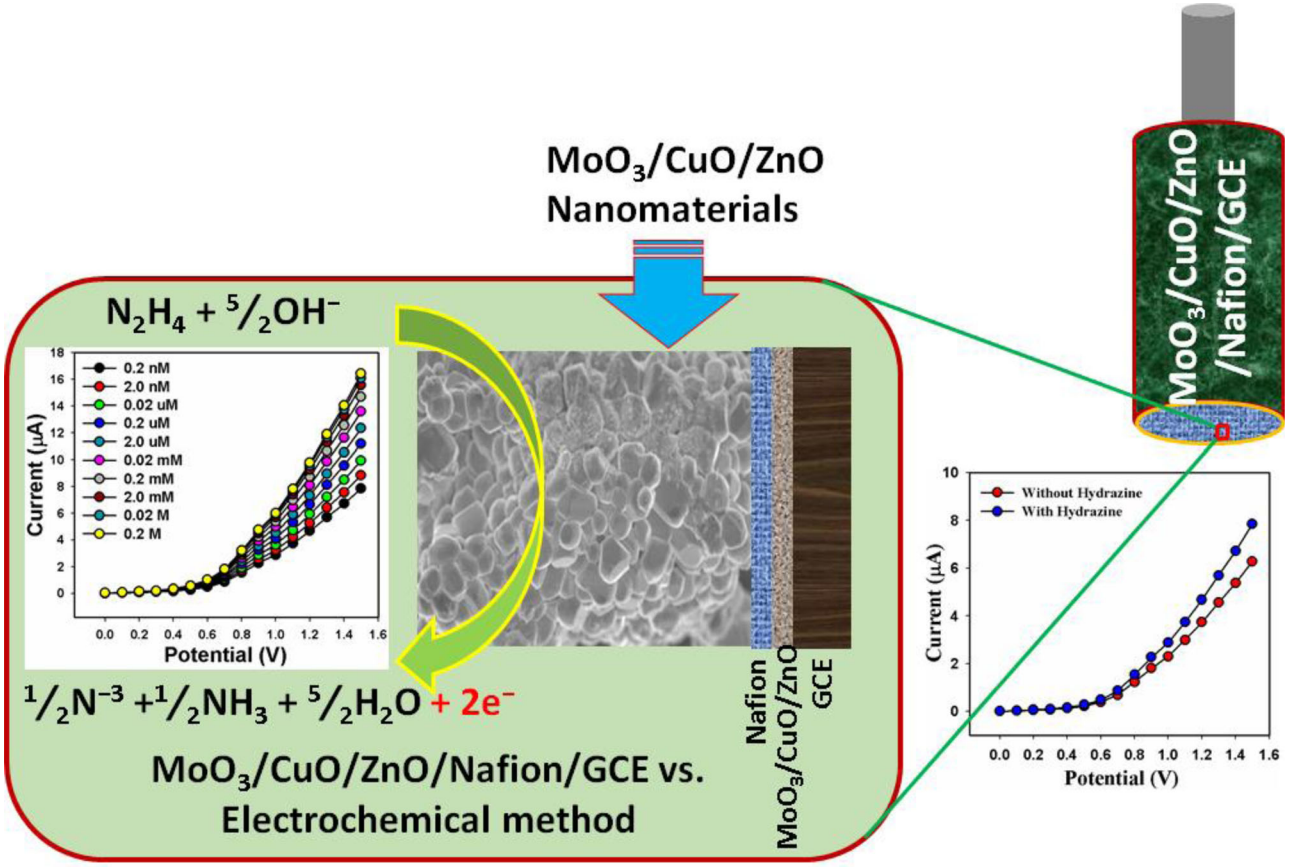

SCHEME 1 Proposed detection mechanism of HZ using MoO_3/CuO/ZnO nanocomposite materials /Nafion/GCE sensor probe assembly by electrochemical approach

presented in Figure 3A. The resultant current intensity for the MoO_3/CuO/ZnO nanomaterials/GCE is slightly higher than that of the bare-GCE, which proves the excellent electro-chemical property of the MoO_3/CuO/ZnO nanocomposite materials. In the presence of HZ in PBS, a noticeable increase in the current response implies the HZ sensing ability with the developed MoO_3/CuO/ZnO nanomaterials/GCE sensor. Electrochemical responses for HZ (1.0 μM; 25.0 μL) in 5.0 mL of PBS solutions using the MoO_3/CuO/ZnO nanomaterials coated GCE (blue dotted), and MoO_3/CuO/ZnO nanomaterials coated GCE (red-dotted) without HZ as working electrodes are measured and given in Figure 3B. In the presence of HZ, a recognizable increase in the current response with the MoO_3/CuO/ZnO nanomaterials/GCE sensor probe compared to MoO_3•CuO•ZnO nanomaterials/GCE (without HZ) is observed, which implies the HZ sensing ability with the developed MoO_3/CuO/ZnO nanomaterials/GCE sensor probe. Figure 3C demonstrates the current variations for different concentration (0.2 nM to 0.2 M) of aqueous HZ solution in the voltage range 0.0 to +1.5 V. It is seen that with the increasing concentration of HZ, the current is significantly increased, that means oxidation is taking place here. A calibration plot is plotted from low to high concentration of HZ (0.2 nM to 0.2 M) and presented in the Figure 3D. For the determination of the sensor analytical parameters, a broad range of the analyte concentrations (0.2 nM ~ 0.2 M) was measured from the lower to higher potential (0.1 to +1.5 V). From the various concentrations of HZ, the linear calibration and magnified calibration curve at +1.1 V were plotted (Figure 3D). Aqueous solutions of HZ (0.2 nM to 2.0 mM) were taken to select the detection limit of the proposed MoO_3/CuO/ZnO nanomaterials/GCE sensor probe. The calibration plot (at +1.1 V) current vs. concentration for the full concentration range is given in Figure 3D. Very high sensitivity value (11.8 $\mu AmM^{-1}\ cm^{-2}$) and LOD as 0.19±0.02 nM were calculated from the calibration plot. LOQ is also calculated as 0.63 nM from the calibration curve. The LDR of the anticipated sensor was obtained from the calibration plot that is 0.2 nM to 2.0 mM (r^2: 0.9813). It is also drawn from the current versus log-conc. of HZ and presented in the Figure 3D (inset).

Sensor current response (12s) is also measured against the response time with Current-Time plot by electrometer and presented in the Figure 4A. It is clearly shown

Full article
doi.org/10.1002/elsa.202100031
Chemistry Europe
European Chemical Societies Publishing

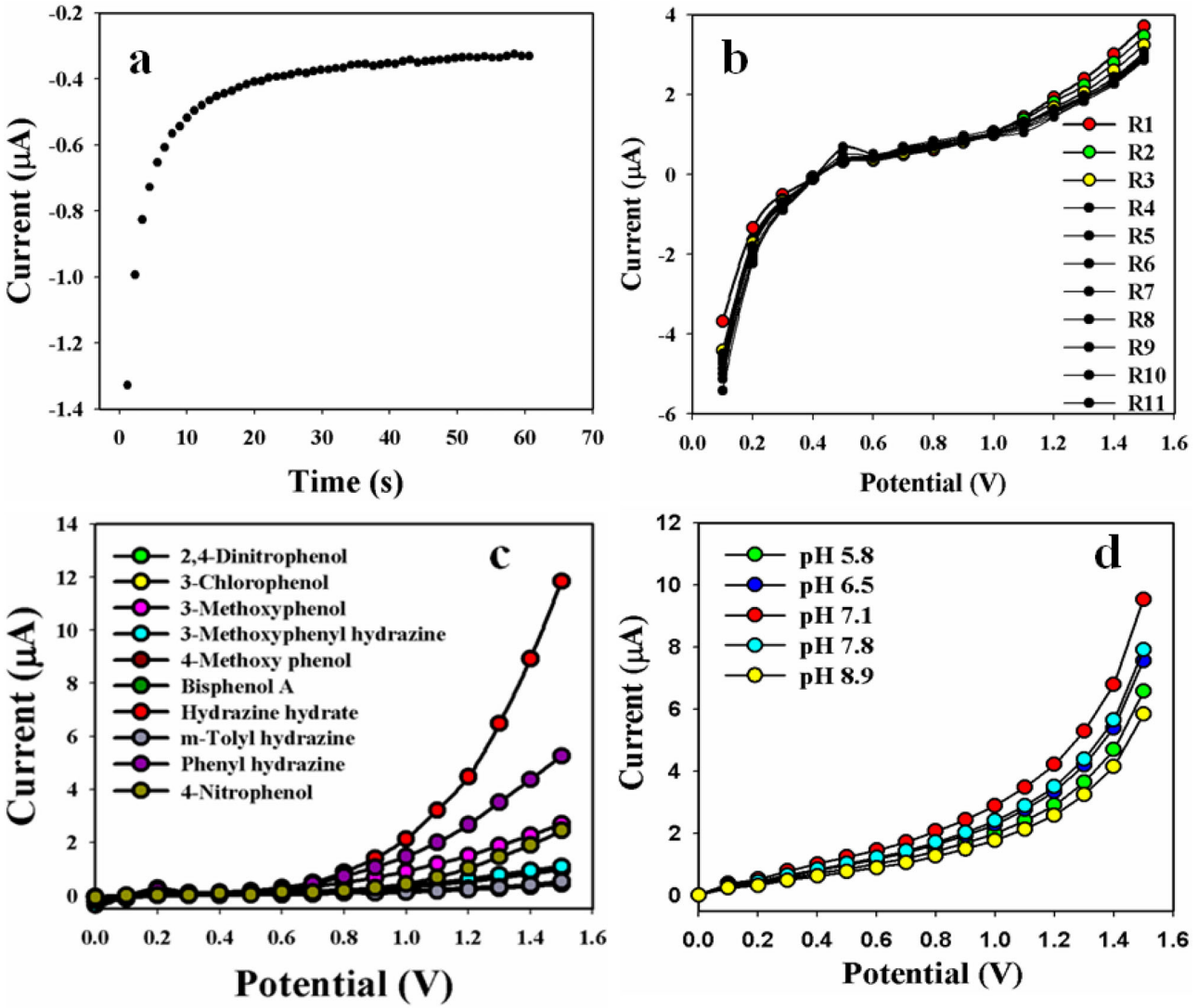

FIGURE 4 Optimization of HZ sensor. (A) Response time for MoO_3/CuO/ZnO/GCE (with HZ), (B) Repeatability using same working electrode; potential range: 0 to +1.5V (concentration of the analyte: 0.1 μM; Volume of the analyte: 25.0 μL; 0.1 M PBS at pH 7.1), (C) Selectivity study of electrochemical responses with various interferences (10 analytes), and (D) pH effect on sensor response during HZ detection

that the current response is stable and saturated after 12 s of response time, which indicates that the sensor is saturated. Figure 4B represents repeatability of the electrochemical responses with the as grown MoO_3/CuO/ZnO nanomaterials coated GCE towards HZ solutions (25.0 μL of 0.1 μM) where same working electrodes were used in run R1~R11 under identical conditions. Almost same current responses in 11 repeated experiments confirm the excellent repeatability of the sensor. Figure 4C demonstrates the current responses with several toxic chemicals (10 analytes), where HZ solution (red-dotted) gave the best response with the MoO_3/CuO/ZnO nanomaterials coated GCE surface. In this selectivity study we have added 1.0 μM; 25.0 μL of each analyte in 5.0 mL of PBS (pH 7.1). The electrochemical response obtained for HZ compared to other analytes is noticeably high which indicates that the sensor works selectively for HZ. It was also noticed that, from dilute (0.2 nM) to concentrated (0.2 M) solution of the HZ, the current response decreases gradually. In this approach, it is optimized the pH for the detection of HZ with MoO_3/CuO/ZnO nanomaterials coated GCE sensor probe by electrochemical method. It is very important and essential to find out the optimum pH in which the produced working electrode is more electrochemical active. Therefore, the fabricated working electrode MoO_3/CuO/ZnO nanomaterials coated GCE sensor probe assembly was investigated in various buffer system (pH 5.8, 6.5, 7.1, 7.8, and 8.9). It was found that the modified electrode with MoO_3/CuO/ZnO nanomaterials coated GCE sensor probe was highly active and given the higher response at the pH 7.1 compare to the other buffer systems, which was illustrated in Figure 4D. Therefore, it was kept

Full article
doi.org/10.1002/elsa.202100031
Chemistry Europe
European Chemical Societies Publishing

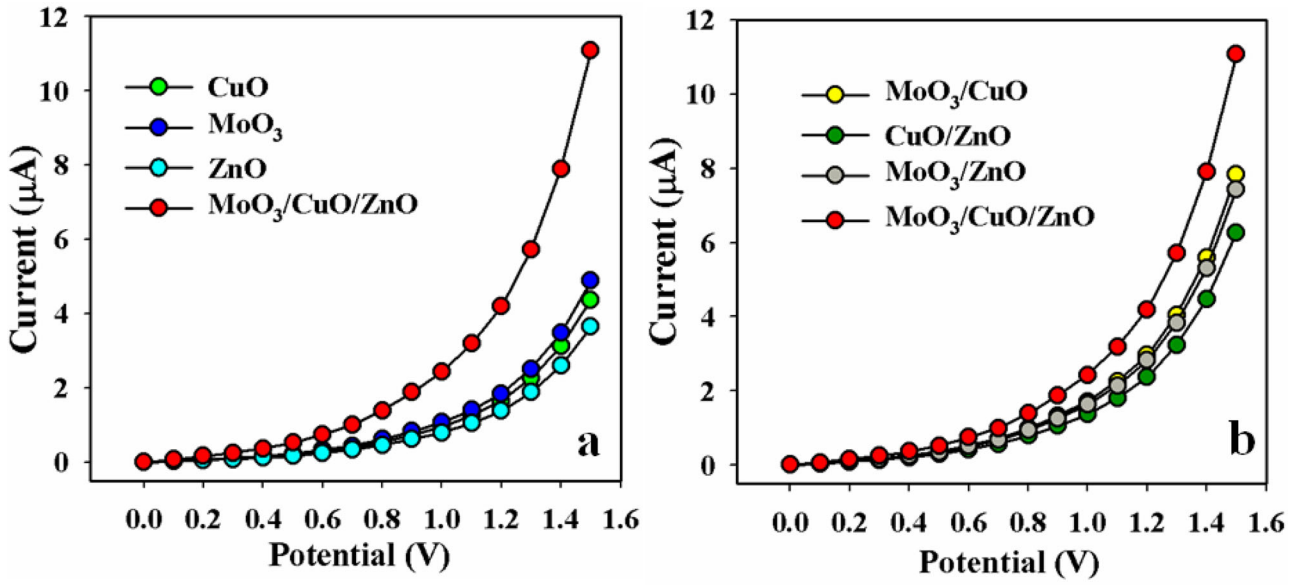

FIGURE 5 Control experiment has been performed by electrochemical method for MoO_3/CuO/ZnO/Nafion/GCE sensor probe with their single and binary oxides. Potential range: 0 to +1.5V; Hydrazine: 0.1 μM; Volume of the analyte: 25.0 μL; 0.1 M PBS at pH 7.1. (A) Electrochemical performance of single metal oxides with ternary metal oxide; and (B) Electrochemical response of binary and ternary metal oxides

constant the pH at 7.1 throughout the HZ measurement with MoO_3/CuO/ZnO nanomaterials coated GCE sensor probe in the sensor study in this investigation.

In this analysis, a control experiment has been performed with their single and binary composites and finally compared with the ternary metal oxides, MoO_3/CuO/ZnO. These experiments have been performed in the identical condition such as potential range: 0 to +1.5V; hydrazine analyte concentration: 0.1 μM; analyte volume: 25.0 μL; 0.1 M PBS at pH 7.1. The hydrazine sensor response is exhibited higher for MoO_3/CuO/ZnO nanomaterials/Nafion/GCE sensor probe compared to their single oxides such as MoO_3/Nafion/GCE, CuO/Nafion/GCE, and ZnO/Nafion/GCE, which is presented in Figure 5A. The similar investigation has been carried out in identical conditions for their binary oxides such as MoO_3/CuO nanomaterials/Nafion/GCE, MoO_3/ZnO/Nafion/GCE, and CuO/ZnO nanomaterials/Nafion/GCE. The result has been also compared and presented in Figure 5B. It is observed that the MoO_3/CuO/ZnO/Nafion/GCE sensor probe exhibited the highest performance compared to their binary sensor probes. Therefore, MoO_3/CuO/ZnO nanomaterial presented here the improved performance in the detection of hydrazine owing to the active and large surface area, which raised the conductivity remarkably as well as current responses in MoO_3/CuO/ZnO/Nafion/GCE sensor probe during electro-chemical analysis compared to their single and binary oxides individually.

The usual regions of MoO_3/CuO/ZnO nanomaterials/Nafion/GCE dispersed on the surface could enhance the capability of MoO_3/CuO/ZnO nanomaterials to take more O_2 species providing more resistances in PBS system. From the literature review, HZ was determined using different chemical techniques.[23–33,53–65] Here, we report the determination of HZ by ternary metal oxides using the current versus voltage technique at room conditions. The analytical outcomes of various electrochemical techniques for the quantification of HZ are given in Table 2.

4 | ELECTROCHEMICAL CHARACTERIZATION OF MoO_3/CuO/ZnO/NAFION/GCE PROBE BY CV AND EIS

Here, the fabricated MoO_3/CuO/ZnO nanomaterials/Nafion/GCE sensor probe was electrochemically characterized by using conventional CV as well as EIS techniques. Before recommending modified MoO_3/CuO/ZnO nanomaterials/Nafion/GCE as an efficient sensor probe material for the detection of selective HZ, it is important to unveil what are the electrochemical redox as well as impedance properties of MoO_3/CuO/ZnO nanomaterials in MoO_3/CuO/ZnO nanomaterials/Nafion/GCE sensor probe assembly. For this purpose, at first, GCE was fabricated by immobilizing MoO_3/CuO/ZnO nanomaterials with the help of conducting coating nafion binder. Here, three electrodes system was used in electrochemical analysis, where Ag/AgCl (Saturated KCl), MoO_3/CuO/ZnO nanomaterials/Nafion/GCE, and Pt was used as reference, working, and counter electrode respectively. The results

TABLE 2 Comparative study of the outcomes of various electrochemical techniques for the quantification of HZ with various sensor matrixes

Electrode fabrication	Method	Medium	pH	DL (μM)	LDR (μM)	Sensitivity (μAmM^{-1} cm^{-2})	Reference
HPIMBD/MWCNT/GCE	Amperometry	PBS	7.0	1.1	4.0-32.9	1.6×10^{-5}	[53]
MnO_2/GO/GCE	Amperometry	PBS	7.0	0.16	–	1.007	[54]
Ag/ZIF-8/CPE	Amperometry	NaOH	–	1.57	6-5000	5.446	[55]
TiO_2-Pt NFs/GCE	Amperometry	PBS	7.0	0.142	1.0 mM	4.42	[56]
CM-MWCNT modified GC	Amperometry	PBS	8.0	1.4	2-44	2.29	[57]
NiHCF modified graphine	Amperometry	$NaNO_3$	7.0	1.0	2.4-8200	1.13	[58]
C@ZnO nanorod array	Amperometry	PBS	8.0	0.1	0.1-3.8	–	[59]
CGA modified GC	CA	PBS	7.5	–	50-11000	–	[60]
PtNPs/TiO_2NSs/GCE	CA + CV	PBS	7.0	2.0	20-900	1.874	[61]
AuNPS/PDTYP/MWCNTS/GCE	CV	PBS	8.0	0.6	2.0-130	–	[62]
O-AP modified GC	CV	PBS	9.0	0.5	2.0-20.0	0.016	[63]
FePc/Au	CV + OSWV	PBS	7.0	5.0, 11.0	13-92	1.62×10^{-5}	[64]
Au/PPy/GC	DPV	PBS	7.0	0.20	5-200	1.26	[65]
Co-ZSM-5	I-V	PBS	7.0	9.10	0.01 nM-0.01 mM	0.0316	[66]
CoS_2–CNT NCs	I-V	PBS	7.0	0.1 nM	0.1 nM-1.0 mM	0.00443	[67]
MoO_3/CuO/ZnO nanomaterials/Nafion/GCE	*I-V*	PBS	7.1	0.19 ± 0.02 nM	0.2 nM – 0.02 M	11.8	This work

*BDD: Boron-doped diamond, CA: Chronoamperometry, CGA: Chlorofenic acid, CM: Curcumin, CNTs: Carbon nano tubes, CV: Cyclic voltametry, FePC: Iron Pathalocyamine, DPV: Differential pulse voltametry, HPIMBD: 4-((2-hydroxyphenylimino)methyl)benzene-1,2-diol, MWCNT: Multiwalled carbon nano tubes, NCs: Nanocomposites, NiHCF: Nickel hexacyanoferrate, NFs: Nano fibers, NPs: Nanoparticles, NSs: Nano sheets, OSWV: Ostero young square wave voltametry, PPy: Polypyrrole, PBS: Phosphate buffer solution, LSV: Linear sweep voltametry.

of CV response in ferricyanide solution redox couple $[Fe(CN)_6]^{3-/4-}$) are shown in Figure 6A. Here, the electron transfer activity is measured within the bare GCE and coated MoO_3/CuO/ZnO nanomaterials/Nafion/GCE by CV method in 5.0 mM $[Fe(CN)_6]^{3-/4-}$ solution (Figure 6A). The MoO_3/CuO/ZnO nanomaterials/Nafion/GCE exhibited good oxidation and reduction peaks at +0.39 V and +0.12 V, respectively. However, bare GCE exhibited a little response in the identical measurement compared to fabricated MoO_3/CuO/ZnO nanomaterials/Nafion/GCE. This indicates that MoO_3/CuO/ZnO nanomaterials significantly enhanced the electron transfer ability of the MoO_3/CuO/ZnO nanomaterials/Nafion/GCE.[68–70] This further confirms results obtained in CV, where MoO_3/CuO/ZnO nanomaterials/Nafion/GCE [Figure 6A (red-line)] exhibited the higher conductance as compared to bare GCE [Figure 6A (blue-line)]. In this approach, EIS is very useful in evaluating electron mobility on the electrode-solution interface and resistivity of prepared MoO_3/CuO/ZnO nanomaterials toward current. Therefore, it was carried out EIS test to further confirm the electrochemical characterization of bare GCE as well as coated MoO_3/CuO/ZnO nanomaterials/Nafion/GCE. Faster electron mobility is expected on the MoO_3/CuO/ZnO nanomaterials/Nafion/GCE in case of effective fabrication of MoO_3/CuO/ZnO nanomaterials onto GCE. The diameter of the semicircle in EIS represents the charge-transfer resistance (R_{CT}) at the surface of the MoO_3/CuO/ZnO nanomaterials /Nafion/GCE electrode.[71–73] As presented in Figure 6B, the bare GCE electrode displayed the higher resistance compared to the MoO_3/CuO/ZnO nanomaterials/Nafion/GCE in a solution containing 5.0 mM ferricyanide (0.1 M PBS; pH at 7.1). This shows that MoO_3/CuO/ZnO nanomaterials/Nafion/GCE has enhanced the charge-transfer ability of the modified sensor surface. This is also an indication that the conductivity of the GCE has greatly increased due to enhanced electron transfer properties of fabricated MoO_3/CuO/ZnO nanomaterials with GCE.[74–76] The complex plane plots displayed in Figure 6B (red-line) indicates that in 0.1 M PBS/$K_3[Fe(CN)_6]$, the MoO_3/CuO/ZnO nanomaterials/Nafion/GCE exhibited less capacitive current as well as lower impedance compared unmodified bare GCE electrode [Figure 6A (blue-line)]. The less capacitive nature with less impedance of the MoO_3/CuO/ZnO nanomaterials /Nafion/GCE sensor suggests the electron-transfer ability of the MoO_3/CuO/ZnO nanomaterials/Nafion/GCE electrode was improved in presence

Full article
doi.org/10.1002/elsa.202100031
Chemistry Europe
European Chemical Societies Publishing

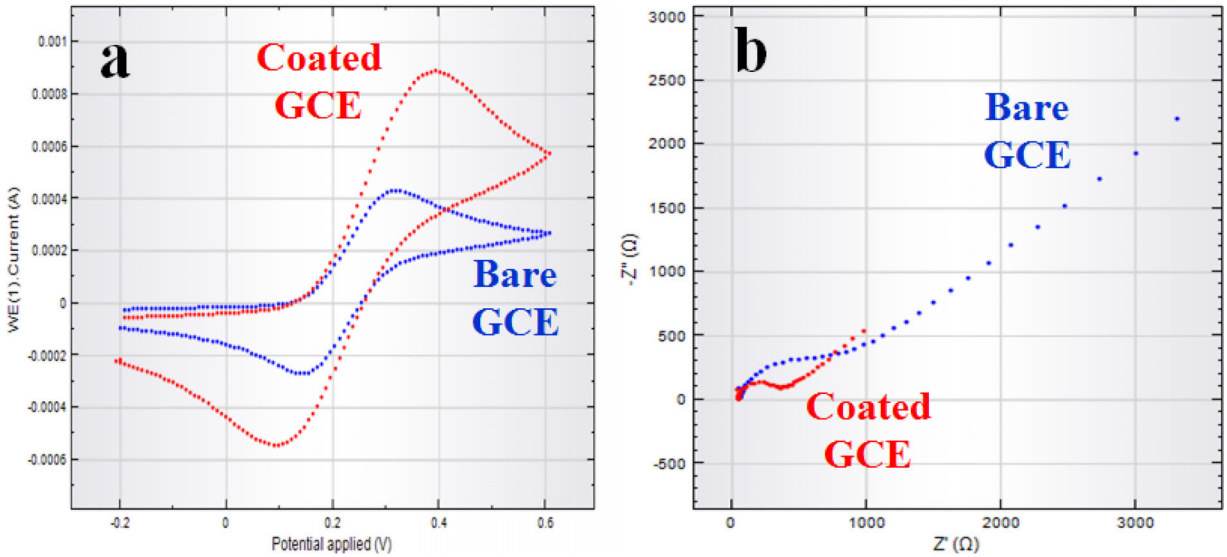

FIGURE 6 Electro-chemical characterization for MoO_3/CuO/ZnO/Nafion/GCE. Comparison of (A) Cyclic voltammetry of bare GCE (blue-line) and (B) Nyquist plots (EIS) (red-dotted) of MoO_3/CuO/ZnO/Nafion/GCE at pH 7.1 in 0.1 M PBS (5.0 mM $[Fe(CN)_6]^{3-/4-}$)

TABLE 3 Real sample analyses by MoO_3/CuO/ZnO nanomaterials/Nafion/GCE system with electrochemical method

	Current (μA)				
Real samples	**Run 1**	**Run 2**	**Run 3**	**Average**	**Concentration of HZ (nM)**
Industrial water	1.5852	2.6585	2.7889	2.3442	0.0605
Plastic baby bottle	0.7338	0.6087	0.5812	0.6412	0.0165
Plastic bottle	1.3495	1.1798	1.1309	1.2200	0.0315

of MoO_3/CuO/ZnO nanomaterials coating, while the MoO_3/CuO/ZnO nanomaterials were bonded with 5% nafion onto the surface of GCE. Thus, such a modified electroactive property of the GCE suggests that the sensor probe of MoO_3/CuO/ZnO nanomaterials has improved the electro-chemical process at the time of EIS evaluation (Figure 6B).

4.1 | Real sample analysis by MoO_3/CuO/ZnO nanomaterials/GCE electrode

To substantiate the validity of the developed sensor, the MoO_3/CuO/ZnO nanomaterials/GCE had been used as WE to determine HZ in effluent-water collected from the industrial ETP, Jeddah, Saudi Arabia as well as in the extract collected from plastic bottle and plastic baby bottle from different companies. For this purpose, we used the standard addition method to check the precision of the HZ detection in aqueous samples. Here, the definite amount (~25.0 μL) of aqueous samples of various concentration along with the equivalent amount of real samples were mixed and analyzed in 0.1 M PBS (5.0 mL) by the MoO_3/CuO/ZnO nanomaterials/GCE working electrodes. Table 3 shows the findings, which exhibited that the MoO_3/CuO/ZnO nanomaterials/GCE modified sensor worked in the quantitative detection of HZ by means of electro-chemical technique. In accordance with the results, we can conclude that the electrochemical approach is suitable, reliable and appropriate in terms of real sample analyses with the help of ternary MoO_3/CuO/ZnO nanomaterials/Nafion/GCE system.

5 | CONCLUSIONS

In this work, MoO_3/CuO/ZnO nanomaterial has been synthesized by means of the co-precipitation technique. Nanomaterial has been characterized with the help of XRD, SEM, EDS, CV, EIS, and Zetasizer. Particle size was determined by XRD which was around 26.5 nm. Toxic chemical, HZ sensor was developed based on the MoO_3/CuO/ZnO nanomaterials fabricated flat-GCE electrode with 5% nafion, it is exhibited the higher sensitivity as well as good selectivity toward HZ sensing implication in various interfering ions or chemicals. With MoO_3/CuO/ZnO/GCE electrode probe, it is significantly employed as a chemical

Full article
doi.org/10.1002/elsa.202100031
Chemistry Europe
European Chemical Societies Publishing

sensor probe for selective HZ detection. The MoO_3/CuO/ZnO/GCE sensor probe for HZ exhibits higher sensitivity as well as very low LOD with short response for a wide linear range of concentration in short response time (12s). This method is promising as an attractive technique in developing efficient chemical sensor probe with ternary metal oxides for the detection of environmental toxins.

6 | EXPERIMENTAL SECTION

6.1 | Materials and methods

Molybdenum(II) chloride, $MoCl_2$ (Sigma Aldrich, Germany), Zinc Nitrate, $Zn(NO_3)_2$•$6H_2O$ (MERCK, India), Copper Chloride, $CuCl_2$•$3H_2O$ (AR, BDH), Sodium Carbonate, Na_2CO_3 (AR, BDH), Sodium Hydroxide, NaOH (AR, BDH) were purchased and used without further purification. 2,4-dinitrophenol, 3-chlorophenol, 3-methoxyphenol, 3-methoxyphenyl hydrazine, 4-methoxy phenol, bisphenol A, hydrazine hydrate, m-toly hydrazine, phenyl hydrazine, 4-nitrophenol, ethanol, disodium phosphate, monosodium phosphate, nafion (5% ethanolic solution) are used in this present work without any further purification and purchased from Sigma-Aldrich Company (USA).

The structural characterization and particle size determination of the nanomaterial was performed by measuring XRD. With the help of a Bruker-AXD advance laboratory diffractometer, XRD was measured by using a Cu Kα. The diffraction patterns at a measurement rate of 10 s/step, and within the 2θ angle ranging 20° to 90° were recorded in the step scan mode at 0.05 steps. For obtaining SEM images and for performing elemental composition analysis of the nanocomposites, Hitachi S-4800 SEM with EDS has been used. Elemental distributions of different samples were confirmed by the EDS spectrum. Hydrodynamic size as well as zeta potential has been measured by Zetasizer Nanoseries (Nano-ZS90). Electrochemical measurements were performed with MoO_3/CuO/ZnO nanomaterials coated GCE using a Keithley electrometer at room conditions. Additionally, for the MoO_3/CuO/ZnO fabricated GCE sensor probe characterization, cyclic voltammogram and electrochemical impedance spectroscopy were investigated with Autolab potentiostat in room conditions.

6.2 | Synthesis MoO_3/CuO/ZnO nanomaterials

Ternary MoO_3/CuO/ZnO and their single and binary metal oxides were synthesized by a simple co-precipitation method. 0.25 $moldm^{-3}$ solutions of three metal salts, $MoCl_2$, $Zn(NO_3)_2$•$6H_2O$, $CuCl_2$•$3H_2O$ and 0.5 $moldm^{-3}$ Na_2CO_3 solution were prepared in distilled water. First of all, metal salt solutions were taken in a beaker having the same volume (50.0 mL each) ratio and stirred constantly for approximately 15 minutes. Then the solution of Na_2CO_3 has been added drop wise, slowly with agitation, until the formation of no more precipitate. The resultant mixture was stirred for a further 1 h at 45 °C with continuous stirring. Upon completion of the reaction, the white metal carbonate precipitate was separated from the solution by means of centrifugation, then washed couple of times with deionized water and finally dried at 120 °C in an oven for 1 h. By using a mortar and pestle, the precipitate was crushed into powder. Then the prepared sample was calcined by using a muffle furnace at a temperature of 600 °C for 3 h. The calcinations converted the carbonates of the sample into their oxides. The overall reactions are provided here

$$(Mo^{2+} + Cl^-) + (Na^+ + CO_3{}^2-) + HOH \rightarrow MoCO_3 \bullet (OH)_2 + CO_2 + (Na^+ + Cl^-)$$

$$(Cu^{2+} + Cl^-) + (Na^+ + CO_3{}^2-) \rightarrow CuCO_3 \bullet (OH)_2 + (Na^+ + Cl^-)$$

$$(Zn^{2+} + NO_3{}^-) + (Na^+ + CO_3{}^2-) \rightarrow ZnCO_3 \bullet (OH)_2 + (Na^+ + NO_3{}^-)$$

$$MoCO_3 \bullet (OH)_2 \rightarrow MoO_3 + CO_2$$

$$CuCO_3 \bullet (OH)_2 \rightarrow CuO + CO_2$$

$$ZnCO_3 \bullet (OH)_2 \rightarrow ZnO + CO_2$$

$$MoO_3 + CuO + ZnO \rightarrow MoO_3 \cdot CuO \cdot ZnO$$

6.3 | Fabrication of GCE using MoO_3/CuO/ZnO nanomaterials

Manufacturing of GCE was performed by the as prepared MoO_3/CuO/ZnO nanomaterials using 5% ethanolic nafion solution as a conducting binder to get a 0.5 mm (approx.) thick film. It was then left at room temperature for 1 hour to attain the dry film onto GCE. In the electro-chemical cell, MoO_3/CuO/ZnO nanomaterials coated GCE is used as WE, Pt-wire is the CE, and aqueous HZ solution in 0.1 M PBS (pH 7.1) is investigated as the working electrolyte. To use as a target analyte, aqueous HZ solution (0.2 M) was diluted to different concentrations (0.02 M to 0.2 nM) by using deionized water (DI) water. The electrochemical measurements were done in 5.0 mL of PBS (pH 7.1). The

sensitivity of the HZ sensor was investigated from the slope of the calibration plot by considering the active surface area of the GCE. By using an electrometer (Keithley, 6517A Electrometer, USA) simple electrochemical technique was applied to HZ solutions taking MoO_3/CuO/ZnO nanomaterials/GCE as WE. Characterization of MoO_3/CuO/ZnO nanomaterials fabricated GCE is done with potentiostat in cyclic voltammetry and impedance spectroscopy by using three electrode systems such as MoO_3/CuO/ZnO nanomaterials/Nafion/GCE, Pt-wire, Ag/AgCl (Sat. KCl) as WE, CE and RE respectively.

ACKNOWLEDGEMENTS

Md Abdus Subhan acknowledged Fulbright USA for Fulbright Visiting Scholar Award (2018-2019) during his stay at Northeastern University, Boston, MA, USA (https://www.cies.org/grantee/dr-md-abdus-subhan). SUST Research Grant (No. 2020/1/01) is gratefully acknowledged for support. Center of Excellence for Advanced Materials Research (CEAMR), King Abdulaziz University, Jeddah, Saudi Arabia is highly acknowledged for their lab facilities and instrumental supports.

DATA AVAILABILITY STATEMENT

Not Applicable

REFERENCES

1. T. Moeller, *J. Am. Chem. Soc.* **1967**, *5*, 306.
2. M. A. Subhan, T. P. Rifat, P. C. Saha, M. M. Alam, A. M. Asiri, M. M. Rahman, & J. Uddin. *RSC Adv.* **2020**, *10*(19), 11274.
3. M. A. Subhan, P. C. Saha, S. A. Sumon, J. Ahmed, A. M. Asiri, M. M. Rahman & Al-M. Mamun. *RSC Adv.* **2018**, *8*, 33048.
4. M. A. Subhan, S. S. Jhuma, P. C. Saha, M. M. Alam, A. M. Asiri, M. Al-Mamun, S. A. Attia, T. H. Emon, A. K. Azad, M. M. Rahman. *New J. Chem.* **2019**, *43*, 10352.
5. M. A. Subhan, S. S. Jhuma, P. C. Saha, J. Ahmed, A. M. Asiri, T. P. Rifat, T. Raihan, A. K. Azad, M. M. Rahman. *J. Environ. Chem. Eng.* **2020**, *8*, 104051.
6. M.A. Subhan, P.C. Saha, Rahman, M. M., Ahmed, J., Asiri, A. M., Mamun, M. A. *New J. Chem.*, **2018**, *42*, 872.
7. M.A. Subhan, P.C. Saha, P. Sarker, M. Al-Mamun, *Res. Chem. Intermed.* **2018**, *44*, 6311.
8. R. Guo, L. Fang, W. Dong, F. Zheng, M. Shen, *Phy. Chem. C.* **2010**, *114*, 21390.
9. M. B. Gholiv, A. Azadbakht, *Electrochim. Acta.* **2011**, *56*, 10044.
10. I. G. Casella, M. R. Guascito, A. M. Salvi, E. Desimoni, *Analytica Chim. Acta.* **1997**, *354*, 333.
11. A. Salimi, L. Miranzadeh, R. Hallaj, *Talanta*. **2008**, *75*, 147.
12. U. P. Azad, V. Ganesan, *Electrochim. Acta.* **2011**, *56*, 5766.
13. J. Ding, T. Liu W. Xu, H. Liao, J. Li, G. Wei, Z. Su, *RSC Adv.* **2015**, *5*, 80719.
14. P. K. Rastogi, V. Ganesan, S. Krishnamoorthi, *Electrochim. Acta.* **2014**, *125*, 593.
15. F. Li, B. Zhang, S. Dong, E. Wang, *Electrochim. Acta.* **1997**, *42*, 2563.
16. J. Li, X. Lin, *Sens. Actuators, B* **2007**, *126*, 527.
17. M.R. Awual, A.M. Asiri, M.M. Rahman, N.H. Alharthi. *Chem. Engineering J.* **2019**, *363*, 64.
18. S. Ivanov, U. Lange, V. Tsakova, V. M. Mirsky, *Sens. Actuator. B Chem.* **2010**, *150*, 271.
19. H. Zhang, J. Huang, H. Hou, T. You, *Electroanalysis*. **2009**, *21*, 1869.
20. C. B. McAuley, C. E. Banks, A. O. Simm, T. G. J. Jones, R. G. Compton, *Analyst*. **2006**, *131*, 106.
21. B. Haghighi, H. Hamidi, S. Bozorgzadeh, *Anal. Bioanal. Chem.* **2010**, *398*, 1411.
22. B. Sljukic, C. E. Banks, A. Crossley, R. G. Compton, *Electroanalysis*. **2006**, *18*, 1757.
23. S. M. Golabi, H. R. Zare, M. Hamzehloo, *Microchem. J.* **2001**, *69*, 111.
24. A. Safavi, A. A. Ensafi, *Anal. Chim. Acta.* **1995**, *300*, 307.
25. S. Ganesh, Fahmida Khan, M. K. Ahmed, P. Velavendan, N. K. Pandey, U. Kamachi Mudali, *J. Anal. Sci., Meth. and Instr.* **2012**, *2*, 98.
26. A. D. Smolenkov, *Rev. J. Chem.* **2012**, *2*(4), 329.
27. G. Elias, W. F. Bauer, *J. Sep. Sci.* **2006**, *29*, 460.
28. K. R. Rao, R. Rambabu, K. R. Babu, *IJIRSET*. **2013**, *2*(11), 6378.
29. A. Safavi, M. R. Baezzat, *Anal. Chim. Acta*, **1998**, *358*, 121.
30. M.M. Rahman, M.M. Alam, A.M. Asiri. *RSC Adv.* **2018**, *8*, 960.
31. E. C. Olson, *Anal. Chem.* **1960**, *32*, 1545.
32. L. Lauko, R. Hudec, K. Lenghartova, A. Manova, F. Cacho, E. Beinrohr, *Pol. J. Environ. Stud.* **2015**, *24*(4), 1659.
33. G. E. Collins, S. L. R. Pehrsson, *Analyst*. **1994**, *119*, 1907.
34. M. Sun, J. Guo, Q. Yang, N. Xiao, Y. Li, *J. Mater. Chem. B.* **2014**, *2*, 1846.
35. M.M. Rahman, M.M. Alam, A.M. Asiri, F.A.D.M. Opo. *Sci. Rep.* **2020**, *10*, 20248.
36. M.M. Alam, A.M. Asiri, M.M. Rahman, M.A. Islam. *Surfaces and Interfaces*. **2020**, *19*, 100540.
37. M. M. Rahman, H. B. Balkhoyora, A. M. Asiri, *RSC Adv.* **2016**, *6*, 29342.
38. S.B. Khan, M. Faisal, M.M. Rahman, I.A. Abdel-Latif, A.A. Ismail, K. Akhtar, A. Al-Hajry, A.M. Asiri, K.A. Alamry. *New J. Chem.* **2013**, *37*, 1098.
39. M. Faisal, S.B. Khan, M.M. Rahman, A.A. Ismail· *J. Taiwan Inst. Chem. Eng.* **2014**, *45*, 2733.
40. C. Karuppiaha, S. Palanisamya, S. M. Chena, S. K. Ramarajb, P. Periakaruppan, *Electrochim. Acta.* **2014**, *139*, 157.
41. C.G. Hu, W.L. Wang, S.X. Wang, W. Zhu, Y. Li. *Diamond Relat. Mater.* **2003**, *12*, 1295.
42. C. Hammond, *The Basic of Crystallography and Diffraction*; Oxford University Press; New York, NY, **1997**.
43. D. R. Patil, L. A. Patil, P. P. Amalnerkar, *Bull. Mat. Sci.* **2007**, *30*, 553.
44. M.A. Subhan, P.C. Saha, M.A. Hossain, M.M. Alam, A.M. Asiri, M.M. Rahman, M. Al-Mamun, T.P. Rifat, T. Raihan, A.K. Azad. *RSC Adv.* **2020**, *10*, 30603.
45. M.M. Rahman, J. Ahmed, A.M. Asiri, K.A. Alamry. *New J. Chem.* **2020**, *44*, 13018.
46. M.M. Rahman, M.M. Alam, A.M. Asiri. *New J. Chem.* **2018**, *42*, 10263.
47. M.M. Rahman, H.M. Marwani, F.K. Algethami, A.M. Asiri. *Material Express* **2017**, *7*, 169.

48. M.M. Rahman, V.G. Alfonso, F. Fabregat-Santiago, J. Bisquert, A.M. Asiri, A.A. Alshehri, H.A. Albar. *Microchim. Acta* **2017**, *184*, 2123.
49. T. Ahmad, I.A. Wani, O.A. Al-Hartomy, A.S. Al-Shihri, A. Kalam, *J. Mol. Struct.* **2015**, *1084*, 9–15.
50. W. Lu, J. Shu, Z. Wang, N. Haung, W. Song, *Mater. Lett.* **2015**, *154*, 33.
51. A. Umar, M.M. Rahman, Y.B. Hahn. *Talanta* **2009**, *77*, 1376.
52. A. Umar, M.M. Rahman, S.H. Kim, Y.B. Hahn. *Zinc oxide nanonail based chemical sensor for hydrazine detection*, Chemical Communication, **2008**, 166.
53. H. R. Zare, Z. Shekari, N. Nasirizadeh, A. A. Jafari, *Catal. Sci. Technol.* **2012**, *2*, 2492.
54. J. Lei, X. Lu, W. Wang, X. Bian, Y, Xue, C. Wang, L Li, *RSC Adv.* **2012**, *2*, 2541.
55. A.S. Maybodi, S. Ghasemi, H.G. Rad. *Sens. Actuat. B: Chem.* **2015**, *220*, 627.
56. Y. Ding, Y. Wang, L. Zhang, H. Zhang, C. M. Li, Y. Lei, *Nanoscale*. **2011**, *3*, 1149.
57. L. Zheng, J. F. Song, *Sens. Actuat. B: Chem.* **2009**, *135*, 650.
58. S. J. R. Prabakar, S.S. Narayanan, *J. Electroanal. Chem.* **2008**, *617*, 111.
59. J. Liu, Y. Lie, J. Jiang, X. Huang, *Dalton Trans.* **2010**, *39*, 8693.
60. S. M. Golabi, H. R. Zare, *J. Electroanl. Chem.* **1999**, *465*, 168.
61. A. R. Fakhari, H. Ahmar, H. Hosseni, S. K. Movahed, *Sens. Actuat. B: Chem.* **2015**, *213*, 82–91.
62. H. M. Nassef, A-E. Radi, C. K. O'Sullivan, *J. Electroanal. Chem.* **2006**, *592*, 139.
63. K.I. Ozoemena, T. Nyokong, *Talanta*. **2005**, *67*, 162.
64. J. Li, X. Lin, *Sens. Actuat. B: Chem.* **2007**, *126*, 527.
65. C. B-McAuley. C. E. Bnaks, A. O. Siman, T. G. J. Jones, R. G. Compton. *Analyst*. **2006**, *131*, 106.
66. M.M. Rahman, B.M. Abu-Zied, A.M. Asiri, *RSC Adv.* **2017**, *7*, 21164.
67. M.M. Rahman, J. Ahmed, A.M. Asiri, I.A. Siddiquey, M.A. Hasnat, *RSC Adv.* **2016**, *6*, 90470.
68. M. Tertiş, A. Florea, A. Adumitrăchioaie, A. Cernat, D. Bogdan, L. Barbu-Tudoran, N. Jaffrezic Renault, R. Săndulescu, C. Cristea, *ChemPlusChem* **2017**, *82*, 561.
69. M.S. Alam, M.M. Rahman, H.M. Marwani, M.A. Hasnat. *Electrochim. Acta* **2020**, *362*, 137102.
70. Z. Mumtarin, M.M. Rahman, M.A. Hasnat. *Electrochim. Acta* **2020**, *346*, 135994.
71. T. Alizadeh, S. Azizi, *Biosens. Bioelectron.* **2016**, *81*, 198.
72. Z. Mumtarin, M.M. Rahman, M.A. Hasnat. *Electrochim. Acta* **2019**, *318*, 486.
73. M.S. Alam, M.F. Shabik, M.M. Rahman, M. del Valle, M.A. Hasnat. *J. Electroanalytical Chemistry* **2019**, *839*, 1.
74. K. Huo, Y. Li, R. Chen, B. Gao, C. Peng, W. Zhang, L. Hu, X. Zhang, P.K. Chu, *ChemPlusChem* **2015**, *80*, 576.
75. J. Ahmed, R.H. Rakib, M.M. Rahman, I.A. Siddiquey, S.S.M. Islam, M.A. Hasnat. *ChemPlusChem* **2019**, *84*, 175.
76. J. Ahmed, M.M. Rahman, I.A. Siddiquey, A.M. Asiri, M.A. Hasnat. *Electrochim. Acta* **2017**, *246*, 597

SUPPORTING INFORMATION

Additional supporting information may be found online in the Supporting Information section at the end of the article.

How to cite this article: Md A. Subhan, P. C. Saha, M. A. R. Akand, A. M. Asiri, M. Al-Mamun, M. M. Rahman. *Electrochem. Sci. Adv.* **2022**, *2,* e2100031. https://doi.org/10.1002/elsa.202100031